T-Type Multi-Inverter Application for Traction Motor Control

Vo Thanh Ha
Faculty of Electrical and Electronic Engineering
University of Transport and Communications
Hanoi, Vietnam
vothanhha.ktd@utc.edu.vn

Pham Thi Giang
Faculty of Electrical Engineering
University of Economics-Technology for Industries
Hanoi, Vietnam
ptgiang@uneti.edu.vn

Vu Hoang Phuong
School of Electrical Engineering
Hanoi University of Science and Technology
Hanoi, Vietnam
phuong.vuhoang@hust.edu.vn

Received: 29 January 2022 | Revised: 10 February 2022 | Accepted: 13 February 2022

Abstract-The structure and principle of the T-type 3-level reverse voltage source that will be fed to three-phase induction motors will be presented in this study. The implementation of Space Vector Pulse Width Modulation (SVPWM) and the math models of the induction motor, the stator currents, and the speed controller design of the electric traction drive system based on Field-Oriented Control (FOC) will be also shown. This three-level T-type inverter in the FOC structure decreases Total Harmonic Distortion (THD) more than the previous two-level inverters. By combining the FOC control structure with the T-type 3-level inverter, the speed and torque responses necessary for railway traction motor load were improved. Finally, Matlab/Simulink will be used to demonstrate the correctness of the T-Type multi-level inverter theory.

Keywords-multilevel inverter; t-type inverter; induction motor; field oriented control; railway traction motor

I. INTRODUCTION

Since the '90s, most asynchronous motors have been replaced, mainly by DC motors. The induction motor outperforms the DC motor in maintenance cost, mechanical stability, and energy efficiency, whereas it can also work in the flux-weakening mode [1-4]. Thus, the induction motor is widely used for railway traction motors. Nowadays, traction electric transportation systems are widely used in developed and developing nations to alleviate traffic congestion in major cities. Traction power systems typically employ big capacity (200kW-300kW), and traction motors are driven from high voltage (25kV, 50Hz) to low voltage (1500V-750V, 50Hz) [5]. Furthermore, since the traction drive system runs at high voltage, a voltage source inverter is required to power the traction motor and assure 100% harmonic distortion of the stator current and, low voltage, standard sine phase voltage, and appropriate controls (torque, speed) for traction electric motor and train operating characteristics. In the control structure of traction power transmission systems, 2-level voltage source inverters with power circuits including 6 semiconductor valves and the PWM SVM technique are often used. However, compared to a multi-level inverter, this 2-level inverter has greater THD [6]. According to [7], the multi-level inverter comprises semiconductor valves and a DC voltage source, and the output voltage is in the form of wavelengths. Therefore, the output voltage of a multi-level inverter may be made sinusoidal with low THD by increasing the number of voltage levels. Currently, clamp diode (NPC), variable capacitor (FC), H-bridge stage (CHB), and T-type multi-level inverters are extensively used in industry and transportation (such as pumps, fans, wind energy, and traction motors for electric trains, electric vehicles, etc.). Based on the literature review [8], the NPC-type multi-level inverter offers benefits over the standard 2-level voltage inverter, such as reduced stator current harmonic distortion and lower TDH voltage. However, because of the NPC's construction, increasing the number of voltage levels will increase the number of diodes and IGBTs, making it impossible to raise further the number of voltage levels [9].

The FC variable-capacitor multi-level inverter has seen a lot of applications. This multi-level inverter has the same construction as the NPC multi-level inverter. Instead of diode transistor valves, a capacitor is used, resulting in different voltages. This benefit allows semiconductor valves to operate without requiring continuous switching. THD is lower than that of the NPC set, resulting in higher efficiency of the FC multi-level inverter than in the NPC set. However, this multi-level inverter costs more than the NPC multi-level inverter [10, 11]. In addition, it has been shown [12, 13] that a multi-level inverter structure of H-bridge cascade (CHB) employs an IGBT semiconductor and a separate DC source (electrolytes). The voltage is provided via several output transformers or

Corresponding author: Vo Thanh Ha

capacitors for industrial applications. This multi-level inverter's power circuit (staged semiconductor phases) is simple to build, replicate, and install in order to increase the number of voltage levels as required. Compared to NPC and FC, a CHB multi-level inverter has this benefit. Furthermore, the CHB multi-level inverter works with medium and high voltages. However, since this multi-level inverter structure requires DC balancing to assure output voltage quality, the control structure must propose a voltage balance management algorithm. Moreover, scientists have been researching the T-Type multi-level inverter because it has more benefits than the CHB structure, such as employing just one DC source and preventing DC voltage imbalance across phases [14, 15]. Besides, authors in [16] shown that the T-type multi-level inverter has the advantage of reducing the number of semiconductor valves and capacitors while increasing the voltage level.

The current article's research, analysis, and assessment focus will be applied to the T-Type three-level inverter for traction motor control power supply in a high-capacity, high-voltage traction power transmission system. In addition, the file-oriented control structure of a traction electric drive system using a T-type 3-level inverter combined with torque speed PI controllers is also provided. Again, this controller is designed so that the responses are accurate.

II. SVM STRUCTURE AND MODULATION OF THE T-TYPE 3-LEVEL INVERTER

A. Control Structure

The 3-phase 3-level T-type inverter structure is developed from the standard 3-phase 2-level voltage source structure. Each phase includes 8 semiconductor valves, such as 4 IGBT valves (SA1-SA4) and 4 diodes (D1-D4). The three-phase design of a three-level T-type converter is shown in Figure 1. The T-type 3-level inverter works on 2 DC capacitors to divide the input voltage into two voltage components $V_{dc}/2$ and create a virtual neutral point. Properly adjusting and switching of the semiconductor valves will give a wire voltage of 5 levels: $-V_{dc}$, $-V_{dc}/2$, 0, $V_{dc}/2$, V_{dc}. Thus, the output phase voltage has the form of 3 levels: $-V_{dc}/2$, 0, $V_{dc}/2$. Based on the working principle of this 3-level T-type inverter, the switching status table is built as shown in Table I.

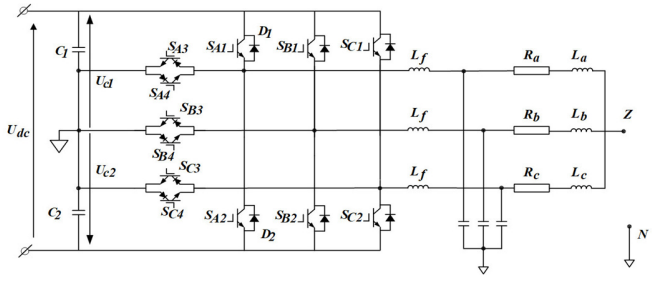

Fig. 1. 3-phase T-type inverter structure power circuit.

TABLE I. T-TYPE 3-LEVEL INVERTER SWITCHING STATUS

Status	V_{out}	SA1	SA2	SA3	SA4
P	$+V_{dc}/2$	ON	OFF	ON	OFF
O	0	OFF	OFF	ON	ON
N	$-V_{dc}/2$	OFF	ON	OFF	ON

B. Pulse Width Modulation SVM

With a multi-level inverse scheme, the number of sub-triangles on the vector plane increases rapidly as the number of levels (M) increases. The calculation becomes more straightforward if we use the system's symmetry in every sixth angle vector space shown on three-six quadrant vector plane coordinate systems (Z1x, Z1y), (Z2x, Z2y), (Z3x, Z3y), where:

$$\begin{cases} v_\alpha = v_A \\ v_\beta = \dfrac{1}{\sqrt{3}}(v_B - v_C) \end{cases} \quad (1)$$

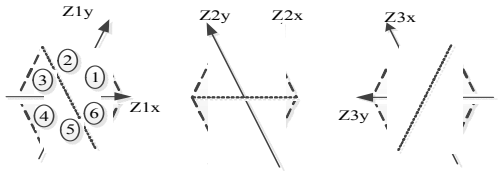

Fig. 2. Coordinate systems (Z1x, Z1y), (Z2x,Z2y) and (Z3x,Z3y).

The number of sub-triangles in the spatial vector diagram will increase as the degree increases. The calculation becomes much easier using the symmetry property of the space vector system in each arc. The coordinate systems (Z1x, Z1y), (Z2x, Z2y) and (Z3x, Z3y) are shown in Figure 2. First, we determine the projection of the desired voltage vector on the upper coordinate system (Z1x, Z1y), (Z2x, Z2y) and (Z3x, Z3y) Then we define three transformation matrices, M1, M2 and M3 described as:

$$M_1 = \begin{bmatrix} 1 & -\dfrac{1}{\sqrt{3}} \\ 0 & \dfrac{2}{\sqrt{3}} \end{bmatrix};\ M_2 = \begin{bmatrix} 1 & \dfrac{1}{\sqrt{3}} \\ -1 & \dfrac{1}{\sqrt{3}} \end{bmatrix};\ M_3 = \begin{bmatrix} 0 & \dfrac{2}{\sqrt{3}} \\ -1 & -\dfrac{1}{\sqrt{3}} \end{bmatrix} \quad (2)$$

According to [6], PWM SVM is performed according to the following calculation steps:

1) Step 1: Locating the Reference Vector

The number of sectors S (S = I, II, ⋯, VI) is determined by Table II.

TABLE II. LOCATING THE HEXAGONS

$z_{1x}.z_{1y} < 0$				$z_{1x}.z_{1y} \geq 0$	
$\mathbf{z_{2x}.z_{2y} < 0}$		$\mathbf{z_{2x}.z_{2y} \geq 0}$		$\mathbf{z_{1x}<0}$	$\mathbf{z_{1x}\geq 0}$
$z_{3x}<0$	$z_{3x}\geq 0$	$z_{2x}<0$	$z_{2x}\geq 0$		
Sec III	Sec VI	Sec V	Sec II	Sec IV	Sec I

2) Step 2: Determining the Duty Cycle

In this step the three nearest vectors are determined based on the three vertices of the modulation triangle, the duty cycle of the three most similar defined vectors is calculated, and the switching states of the semiconductor valves are chosen. With the assumption shown in Figure 3, the sum of the output voltage vector is as follows:

The vector is represented by the vectors in (3):

$$\begin{aligned}\vec{V}_1 &= \vec{p}_1 + m_g(\vec{p}_2 - \vec{p}_1) + m_h(\vec{p}_3 - \vec{p}_1) \\ &= (1 - m_g - m_h)\vec{p}_1 + m_g\vec{p}_2 + m_h\vec{p}_3\end{aligned} \quad (3)$$

$$\begin{aligned}\vec{V}_2 &= \vec{p}_4 + (1 - m_g)(\vec{p}_3 - \vec{p}_4) + (1 - m_h)(\vec{p}_2 - \vec{p}_4) \\ &= (m_g + m_h - 1)\vec{p}_4 + (1 - m_g)\vec{p}_3 + (1 - m_h)\vec{p}_2\end{aligned} \quad (4)$$

The coefficients m_g and m_h are determined as follows:

$$\begin{cases} m_g = z_{1x} - \lfloor |z_{1x}| \rfloor = z_{1x} - k_g \\ m_h = z_{1y} - \lfloor |z_{1y}| \rfloor = z_{1y} - k_h \end{cases} \quad (5)$$

with $k_g = \lfloor |z_{1x}| \rfloor, k_h = \lfloor |z_{1y}| \rfloor$.

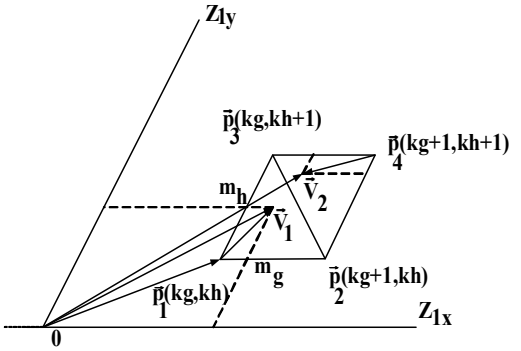

Fig. 3. Synthesizing the output voltage vector from the 3 vertex vectors of the sub-triangle.

3) Step 3: Determining the Switching State

If $k_A = k$, the coefficient k must satisfy this condition: $-\frac{M-1}{2} \le k \le \frac{M-1}{2}$. The coordinates of the state vector in the (a, b, c) coordinate system are given by (6):

$$\begin{bmatrix} k_{1x} \\ k_{1y} \end{bmatrix} \approx \begin{bmatrix} k_{AN} \\ k_{BN} \\ k_{CN} \end{bmatrix} = \begin{bmatrix} k \\ k - k_{1x} \\ k - k_{1x} - k_{1y} \end{bmatrix} \quad (6)$$

Equation (6) shows the relationship between [k_{1x}, k_{1y}] coordinates (i = 1,2,3) and (a, b, c) coordinates.

4) Step 4: Balancing the Voltage on the Two DC Capacitors Using SVM Modulation

For multi-level inverters, voltage balancing for DC capacitors is always a challenge. Although just one DC source is utilized in the T-type inverter construction, voltage imbalance on the two capacitors in series is conceivable for a variety of reasons, including:

- The DC capacitor's value is inaccurate in this case.
- Due to inefficient circuit switching, the discharge and charge times of two capacitors differ.

As a result, DC voltage will deteriorate the harmonic quality of the inverter output voltage, which is impossible. Thus, multi-level inverters in general, and T-type inverters in particular, must address this issue. The steps for balancing the capacitor voltage are:

- Step 1: Measure the voltage on the capacitors Vdc1, Vdc2.
- Step 2: Compare the two voltages.
- Step 3: Discharge voltage on capacitor C1 and charge capacitor C2 if Vdc1 > Vdc2.
- Step 4: Discharge voltage on the capacitor C2 and charge C1 if Vdc2 > Vdc1.

TABLE III. ORDER OF THE VECTOR SWITCHES

Sector	Triangle shape	Switching order	Case of unbalance
1	1	(0 0 0) - (1 0 0) - (1 1 0) – (1 0 0)	Vc1>Vc2
		(-1 -1 -1) – (0 -1 -1) – (0 0 -1) – (0 -1 -1)	Vc2>Vc1
	2	(1 0 0) – (1 0 -1) – (1 -1 -1) – (1 0 -1)	Vc1>Vc2
		(0 -1 -1) - (1 -1 -1) - (1 0 -1) - (1 -1 -1)	Vc2>Vc1
	3	(1 0 0) - (1 1 0) -(1 0 -1) - (1 1 0)	Vc1>Vc2
		(0 -1 -1) - (0 0 -1) - (1 0 -1) - (0 0 -1)	Vc2>Vc1
	4	(1 1 0) - (1 1 -1) - (1 0 -1) - (1 1 -1)	Vc1>Vc2
		(0 0 -1) - (1 0 -1) - (1 1 -1) - (1 0 -1)	Vc2>Vc1

Table III shows the changing of the switching order in sector one to balance the voltage on the capacitor. We follow the same procedure in the remaining sectors. The voltage imbalance between the two capacitors C1 and C2 may be determined using the state table, and control can be used to balance the voltage on the two capacitors.

III. MATHEMATICAL MODELS

A. Mathematical Model of Induction Motor

The FOC approach is used to regulate the induction motor, hence, the induction motor's mathematical model (based on [4]) is:

$$\begin{cases} \dfrac{di_{sd}}{dt} = -\left(\dfrac{1}{\sigma T_s} + \dfrac{1-\sigma}{\sigma T_r}\right) i_{sd} + \omega_s i_{sq} + \dfrac{1-\sigma}{\sigma T_r} + \dfrac{1}{\sigma L_s} u_{sd} \\ \dfrac{di_{sq}}{dt} = -\omega_s i_{sd} - \left(\dfrac{1}{\sigma T_s} + \dfrac{1-\sigma}{\sigma T_r}\right) i_{sq} - \dfrac{1-\sigma}{\sigma} \omega i_m + \dfrac{1}{\sigma L_s} u_{sq} \\ \dfrac{d\psi_{rd}}{dt} = -\dfrac{1}{T_r}\psi_{rd} + \dfrac{L_m}{T_r} i_{sd} \\ \dfrac{d\omega}{dt} = k_\omega \psi_{rd} i_{sq} - \dfrac{z_p}{J} m_L \end{cases} \quad (7)$$

with $\omega_s = \omega + \omega_r = \omega + \dfrac{L_m}{T_r}\dfrac{i_{sq}}{\psi_{rd}}; k_\omega = \dfrac{3}{2}\dfrac{z_p^2 L_m^2}{L_r J}$.

The equation represents the IM's mechanical equation:

$$m_M = m_T + \frac{Jd\omega}{dt} \quad (8)$$

B. Mathematical Model of the Traction Motor Load

Traction motor load includes load torque and drag forces. The drag force of the electric traction motor is a characteristic

quantity for the train's movement, including two main components, essential and auxiliary resistance.

1) Basic Drag

The main factors that cause drag are friction and impact between the wheel and the rails, between the locomotive and the air, and between the locomotive parts. The essential parts of frictional resistance between the bearing and the wheel hub are: rolling resistance, sliding, shock and shock, and air. From the above factors, it can be seen that the factors affecting the essential unit resistance are very complex and, in practice, it is challenging to use theoretical formulas to calculate. Therefore, empirical formulas are often used, related to the square of train speed. The general form of the procedure for calculating essential train resistance is:

$$W_0 = A + BV + CV^2 \text{ (kN)} \quad (9)$$

The primary resistance of the locomotive when operating traction and when running momentum is not equal, so for all types of locomotives, it is necessary to find a formula for calculating separately the two primary resistances, which are the unit essential resistance $\omega_0^{'}$ and the elemental resistance when running momentum $\omega_{0cd}^{'}$. The general formula for calculating the unit resistance of the locomotive is:

$$\omega_0^{'} = 6.37 + \frac{127.5}{0.1.q} + 0.98.\frac{V}{10} + \frac{CA}{0.1.i.q}\left(\frac{V}{10}\right)^2 \quad (10)$$

The basic formula for calculating resistance when running momentum (generally used for locomotives) is:

$$\omega_{0cd}^{'} = 2.4 + 0.1.V + 0.00035.V^2 \quad (11)$$

2) Secondary Drag

Slope resistance is the principal source of secondary drag. Auxiliary resistance differs from elemental resistance: It is less impacted by the locomotive or wagon type. Because route circumstances determine it, the additional damper does not differentiate between locomotives and wagons but is computed per train. The unit ramp resistance is calculated as:

$$\omega_i = \frac{W_i}{(P+Q).g} = 1000.\sin\theta \quad (12)$$

IV. SIMULATION RESULTS

A control structure for traction motors driven by a 3-level T-type inverter is depicted in Figure 4, based on the above findings. The simulation results for electric traction motors using the 3-level T-type inverter and induction motor specifications are shown in Table IV.

TABLE IV. PARAMETER TABLE

Parameters	Symbol	Value
DC voltage	U_{dc}	1000
Frequency of modulation	fs	2000Hz
Power	P_{dm}	270 kW
Rated speed	n_{dm}	2880 rpm
Rated voltage	U_{dm}	400V
Pole pair	P	1
Power factor	cosφ	0.9
Stator resistance	R_s	0.0138Ω
Rotor resistance	R_r	0.00773Ω
Rotor inductance	L_r	0.0078H
Mutual inductance	L_m	0.0077H
Voltage		750 VDC
Maximum speed for the train		80km/h

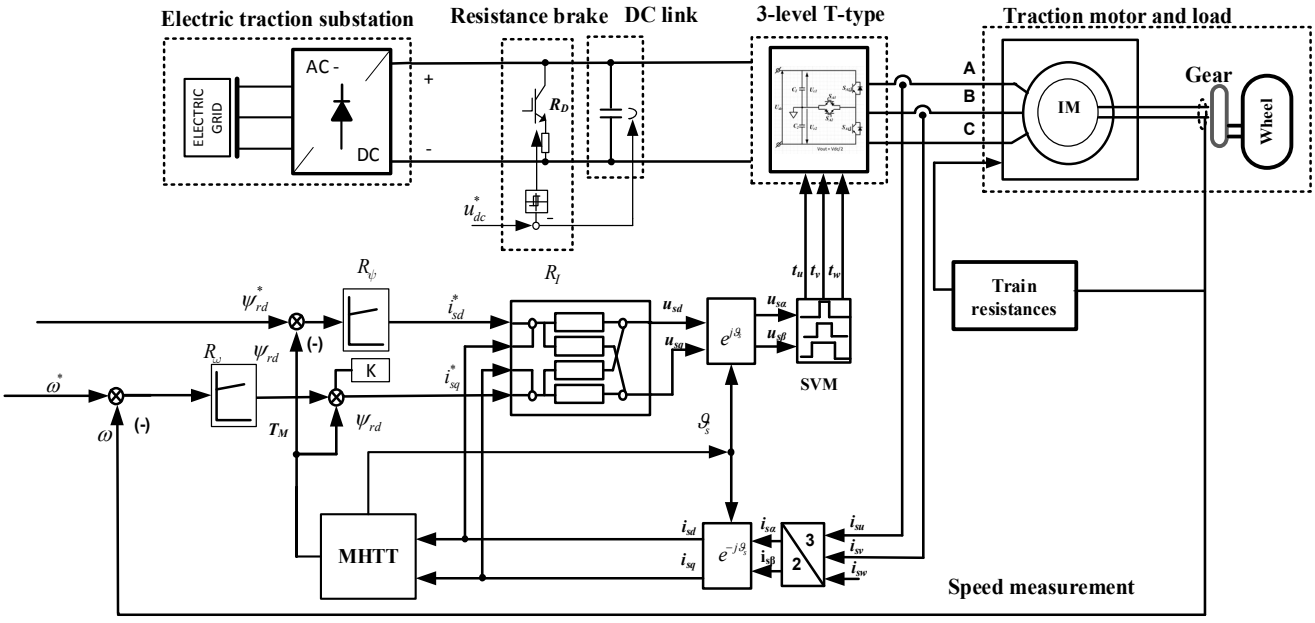

Fig. 4. Control structure of traction motor fed by T-type 3-level inverter.

To evaluate the effectiveness of the 3-level T-type inverter, the stator current controller will be selected as PI in the control structure, with the adjustment parameters chosen as: $K_p = 0.385; T_i = 0.052$. In addition, the speed controller is a PI controller with parameters $K_p = 4.1; T_i = 0.82$.

A. Case 1: Simulation and Evaluation of the 3-Level T-Type Inverter with Two Classic Levels at 50Hz with No Load

The phase voltage response and THD are displayed in Figure 5. Figure 6 depicts the DC voltage response on the two capacitors of a T-type 3-levels inverter. Through the simulation results (Figure 5), it was found that the output voltage of the 3-level T-type inverter has a wavelength with the three required voltage levels. In addition, the current is sinusoidal with lower THD (7.53%) than a two-voltage level inverter (THD = 11.39%). In addition, the difference in DC voltage between the two capacitors is not significant, with the most notable change being Vcmax = 3V (0.6%), demonstrating that the balancing procedure is successful. Furthermore, owing to the voltage balancing technique on capacitors, SVM modulation considerably reduces the voltage imbalance on the two DC capacitors. Consequently, the SVM modulation produces acceptable voltage and current quality with a THD of 7.53%.

B. Case 2: Simulation and Evaluation of Traction Drive System Using the 3-Level T-Type Inverter

Traction electric motor will operate according to the following simulation scenario:

- From t = 0.5s to t=2.3s, the IM is operating at pull process with: $t_{0.5s}$ =0 (km/h), t_{1s}=50 (km/h), and $t_{2.3s}$=73 (km/h).
- From t = 2.3s to t = 4.5s, the IM is operating at coasting process with: $t_{2.3s}$ =73 (km/h), $t_{4.5s}$ =73 (km/h).
- From t = 4.5s to t = 8s, the IM is operating at braking process with: t_{7s} =13 (km/h) and t_{8s}=0 (km/h).

The simulation results are shown in Figure 7.

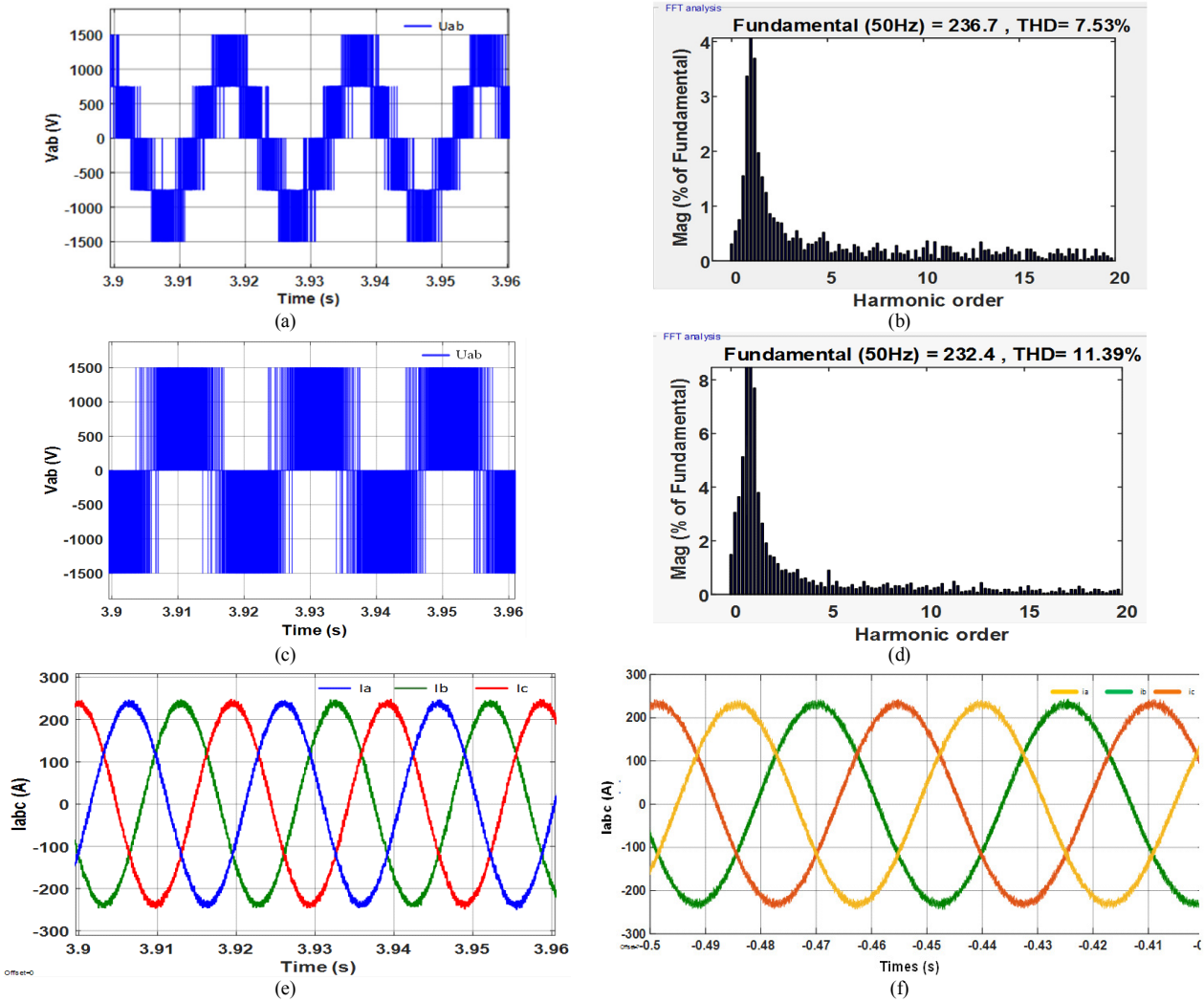

Fig. 5. Line voltage and THD of the T-type multi-level inverter and the classic 2-level inverter. (a), (b) T-type 3-level voltage inverter, (c), (d) inverter 2 voltage levels, (e) 3-phase current response using the 3-level T-type, (f) classic 2-level inverter current response.

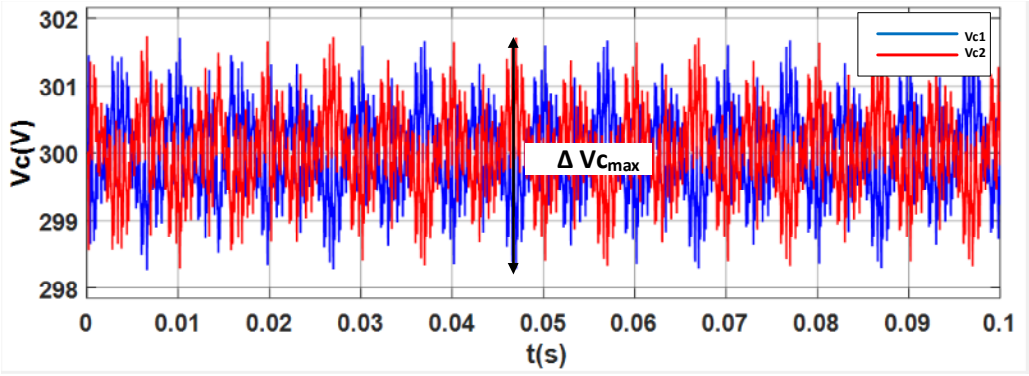

Fig. 6. The DC voltage response on two capacitors of a T-type 3-level inverter.

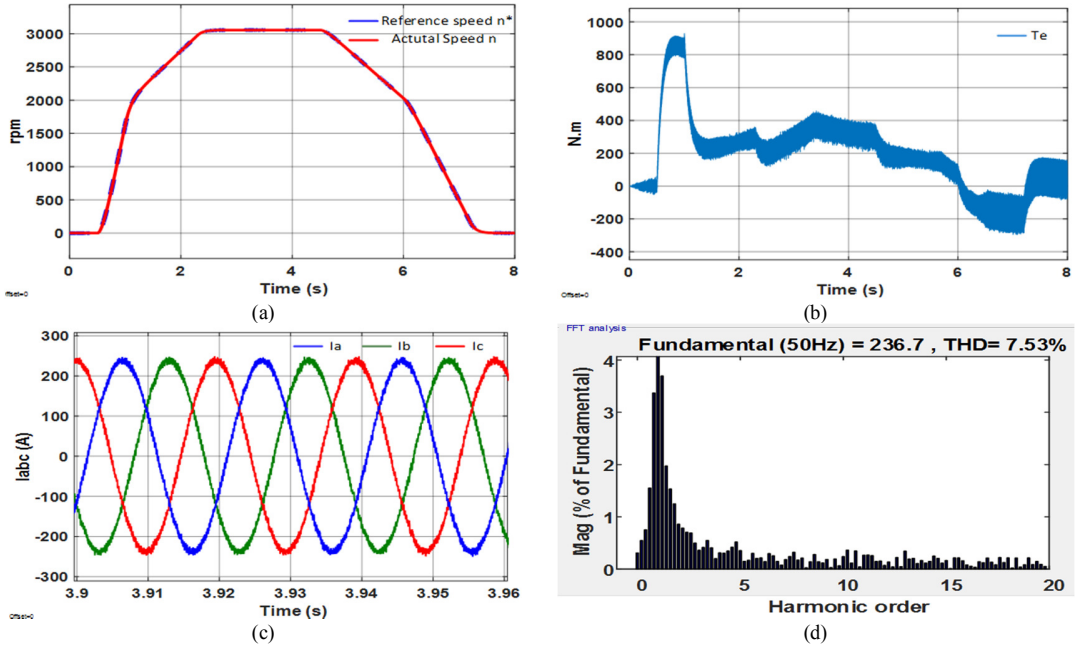

Fig. 7. (a) Speed response, (b) torque response, (c) single phase voltage, (d) TDH when Rr is constant.

Figure 7 shows that the output voltage of the 3-level T-type inverter has a wavelength with the required 3 voltage levels. Furthermore, the current is sinusoidal, resulting in decreased THD. In addition, the torque and speed controllers have been effective. Thus, the actual speed response closely reflects the reference speed response with a rapid reset time. On the other hand, the torque controller provided the required torque at each operating moment of the railway traction drive. As a result, boosting the voltage level and applying a nonlinear control approach to the controllers is a challenge that has to be handled in the future to assure minimal THD and minor torque pulsation.

V. CONCLUSION

The design and assessment of the control structure of a traction motor FOC driven by a 3-level T-type inverter were effectively suggested in this study. According to the simulation results, the harmonic distortion diminishes as the voltage level rises, resulting in increased inverter performance. The design and computation of this multi-level inverter, on the other hand, is complicated, mainly when the number of voltage vectors grows fast with voltage level. Furthermore, since the torque response still exhibits strong torque pulsation, a more straightforward voltage modulation method is required when the power level rises and the torque pulsation reduces. This is a promising area for future research, as methods to enhance the control quality of traction powertrains are developed.

REFERENCES

[1] L. Frederick and G. K. Dubey, "AC motor traction drives—A status review," *Sadhana*, vol. 22, no. 6, pp. 855–869, 1997.

[2] M.-Ş. Nicolae and I.-R. Bojoi, "A control strategy for an induction motor used for vehicular traction and/or positioning systems with variable speeds," in *2012 International Conference on Applied and Theoretical Electricity (ICATE)*, Craiova, Romania, Jul. 2012, pp. 1–6, https://doi.org/10.1109/ICATE.2012.6403425.

[3] A. Fathy Abouzeid *et al.*, "Control Strategies for Induction Motors in Railway Traction Applications," *Energies*, vol. 13, no. 3, Jan. 2020, Art. no. 700, https://doi.org/10.3390/en13030700.

[4] N. P. Quang and J. A. Dittrich, *Vector control of three-phase AC machines*, 2nd ed., vol. 2. Hedelberg, Germany: Springer, 2015.

[5] A. Steimel, *Electric Traction - Motive Power and Energy Supply: Basics and Practical Experience*. Munich, Germany: Oldenbourg Industrieverlag, 2008.

[6] C. M. Van, T. N. Xuan, P. V. Hoang, M. T. Trong, S. P. Cong, and L. N. Van, "A Generalized Space Vector Modulation for Cascaded H-bridge Multi-level Inverter," in *2019 International Conference on System Science and Engineering (ICSSE)*, Dong Hoi, Vietnam, Jul. 2019, pp. 18–24, https://doi.org/10.1109/ICSSE.2019.8823465.

[7] S. Pradhan, "Multilevel Inverter Based Electric Traction Motor," M.S. thesis, National Institute of Technology, Odisha, India, 2013.

[8] N. B. Mohite and Y. R. Atre, "Neutral-Point Clamped Multilevel Inverter Based Transmission Statcom for Voltage Regulation," in *Second International Conference on Emerging Trends in Engineering (SICETE)*, Jaysingpur, India, 2010, pp. 31–35.

[9] F. Z. Peng and J.-S. Lai, "Dynamic performance and control of a static VAr generator using cascade multilevel inverters," *IEEE Transactions on Industry Applications*, vol. 33, no. 3, pp. 748–755, Feb. 1997, https://doi.org/10.1109/28.585865.

[10] J. Rodriguez, S. Bernet, B. Wu, J. O. Pontt, and S. Kouro, "Multilevel Voltage-Source-Converter Topologies for Industrial Medium-Voltage Drives," *IEEE Transactions on Industrial Electronics*, vol. 54, no. 6, pp. 2930–2945, Sep. 2007, https://doi.org/10.1109/TIE.2007.907044.

[11] M. Rezki and I. Griche, "Simulation and Modeling of a Five -Level (NPC) Inverter Fed by a Photovoltaic Generator and Integrated in a Hybrid Wind-PV Power System," *Engineering, Technology & Applied Science Research*, vol. 7, no. 4, pp. 1759–1764, Aug. 2017, https://doi.org/10.48084/etasr.1271.

[12] P. Guerriero *et al.*, "Three-Phase PV CHB Inverter for a Distributed Power Generation System," *Applied Sciences*, vol. 6, no. 10, Oct. 2016, Art. no. 287, https://doi.org/10.3390/app6100287.

[13] Y. Gopal, K. P. Panda, D. Birla, and M. Lalwani, "Swarm Optimization-Based Modified Selective Harmonic Elimination PWM Technique Application in Symmetrical H-Bridge Type Multilevel Inverters," *Engineering, Technology & Applied Science Research*, vol. 9, no. 1, pp. 3836–3845, Feb. 2019, https://doi.org/10.48084/etasr.2397.

[14] D. A. Tuan, P. Vu, and N. V. Lien, "Design and Control of a Three-Phase T-Type Inverter using Reverse-Blocking IGBTs," *Engineering, Technology & Applied Science Research*, vol. 11, no. 1, pp. 6614–6619, Feb. 2021, https://doi.org/10.48084/etasr.3954.

[15] H. P. Vu, D. T. Anh, and H. D. Chinh, "A Novel Modeling and Control Design of the Current-Fed Dual Active Bridge Converter under DPDPS Modulation," *Engineering, Technology & Applied Science Research*, vol. 11, no. 2, pp. 7054–7059, Apr. 2021, https://doi.org/10.48084/etasr.4067.

[16] L. G. Franquelo, J. Rodriguez, J. I. Leon, S. Kouro, R. Portillo, and M. A. M. Prats, "The age of multilevel converters arrives," *IEEE Industrial Electronics Magazine*, vol. 2, no. 2, pp. 28–39, Jun. 2008, https://doi.org/10.1109/MIE.2008.923519.